[29]O. Benary, N. Barash-Schmidt, L. R. Prier, A. H. Rosenfeld, and G. Alexander, UCRL Report No. UCRL-20000 YN (unpublished).
[30]M. M. Block *et al.*, in *Proceedings of the International Conference on Hyperfragments, St. Cergue, Switzerland, 1963* (CERN, Geneva, 1964), p. 63.
[31]B. F. Gibson and M. S. Weiss, Phys. Rev. C 2, 865 (1970).
[32]J. T. Londergan and R. Dalitz, Phys. Rev. C 4, 747 (1971).

PHYSICAL REVIEW C VOLUME 6, NUMBER 3 SEPTEMBER 1972

High-Energy Neutron-Nuclei Total Cross Sections*

Victor Franco
Physics Department, Brooklyn College of the City University of New York, Brooklyn, New York 11210
(Received 28 December 1971; revised manuscript received 8 June 1972)

Total cross sections for collisions between high-energy neutrons and nuclei are calculated by means of the Glauber approximation. Both Woods-Saxon and Gaussian density distributions are assumed for the nuclei. The two distributions yield results which may differ from each other by as much as 15%. For light nuclei harmonic-oscillator wave functions are used. The calculations are compared with measurements for neutron energies above 1 GeV. A simple explanation is given to show why the dependence of the cross sections on the mass number A is greater than $A^{2/3}$. Although the multiple scattering series for a mass-A nucleus contains A terms, it is shown that excellent accuracy is obtained by retaining only approximately $3A^{1/3}$ terms and a geometrical argument leading to this result is given. The ratios of the real to imaginary parts of the hadron-nuclei forward elastic scattering amplitudes are calculated and the decrease of their magnitudes with increasing mass number is explained. The neutron-nuclei data are consistent with little or no regeneration.

I. INTRODUCTION

Some years ago it was predicted[1,2] that double collisions (i.e., collisions with two target nucleons) are more probable than single collisions in high-energy hadron-deuteron scattering at angles away from the forward direction. Since that time a considerable number of experimental studies of hadron-deuteron scattering have been made, and analyses of the measurements have confirmed this prediction.[3-12] Recently a number of analyses of high-energy hadron-nucleus collisions have been based upon the diffraction approximation due to Glauber.[13] This approximation is most accurate for collisions involving small momentum transfers. Consequently it is not unreasonable to expect that high-energy hadron-nucleus total cross sections, which depend only upon the forward elastic scattering amplitudes via the optical theorem, could be calculated quite reliably for a given nuclear model. Such calculations have been carried out for a simple model in which nuclei are described by Gaussian density distributions.[14] Such a model, although quite unrealistic, is very useful because it leads to an analytic expression for the total cross sections which exhibits some qualitative features that are likely to reappear in more realistic calculations.[15] Alternative approaches for calculating neutron-nucleus cross sections are possible using, for example, the optical-model methods of Francis and Watson,[16] Bethe,[16] and of Kerman, McManus and Thaler.[16] The accuracy of the optical model is, however, less satisfactory for calculations of nucleus-nucleus cross sections. The present analysis can be extended to treat nucleus-nucleus collisions.[17]

We have performed analyses of total cross sections in which the explicit multiple scattering form of the Glauber approximation has been retained. We use both a model in which the nuclei have Gaussian density distributions and a model in which the nuclei have Woods-Saxon shapes for the density distributions.[18] (We have also performed the calculations for light nuclei using harmonic-oscillator wave functions.) The quantitative results obtained with the Gaussian and Woods-Saxon models differ by as much as 15%. This seemingly small difference is significant, since recent measurements have uncertainties which are much smaller than 15%. Nevertheless, over the current physical range of nuclei ($A \lesssim 240$) the quantitative results are not grossly sensitive to the nuclear model. Consequently our predictions could serve as a rather severe test of the basic theory. Alternatively, if we have confidence in the theory, our predictions could serve as a test of the reliability of total cross-section measurements. To the degree that the theory is sensitive

to the nuclear parameters, it may serve as an alternative means for determining these parameters. Since quite a number of high-energy neutron-nucleus total cross-section measurements have been made in recent years,[19-30] we have calculated these cross sections and compared them with the data. In addition to studying the neutron-nuclei total cross sections, we have investigated the behavior of the real part of the neutron-nuclei forward elastic scattering amplitude.

In Sec. II we present some basic formulas relevant to neutron-nucleus collisions at high energies. In Sec. III we calculate total cross sections for Woods-Saxon density distributions and for harmonic-oscillator wave functions and compare our predictions with measurements. Cross sections for Gaussian density distributions are discussed in Sec. IV as is the rapidity of convergence of the multiple scattering series. In Sec. V we discuss the A dependence of the cross sections and the study of density distributions by means of cross-section measurements. In Sec. VI we investigate the real parts of the neutron-nuclei forward elastic scattering amplitudes. In the final section we present our calculations for neutron-deuteron cross sections.

II. BASIC FORMULAS

In this section we shall present a few of the basic formulas of the theory. A more complete description of the material is given in Refs. 1 and 13. The forward elastic scattering amplitude for hadron-nucleus collisions may be approximated by[13]

$$F_{ii}(0)=ik\int_0^\infty\left\{1-\left[1-\frac{1}{ik}\int_0^\infty J_0(qb)f(q)S(q)q\,dq\right]^A\right\}b\,db\,, \tag{2.1}$$

where $AS(q)$, the form factor of the nucleus, is given in terms of the single-particle density ρ by

$$S(q)=\frac{4\pi}{q}\int_0^\infty r\sin qr\,\rho(r)dr\,, \tag{2.2}$$

and $f(q)$ is the hadron-nucleon elastic scattering amplitude. The incident momentum is $\hbar k$.

At high energies hadron-nucleon elastic scattering angular distributions exhibit sharp diffraction peaks near the forward direction. They are quite accurately described by amplitudes of the form

$$f(q)=\frac{(i+\alpha)k\sigma_N}{4\pi}e^{-\beta q^2/2}, \tag{2.3}$$

where σ_N is the hadron-nucleon total cross section, α is the ratio of the real to imaginary parts of the forward elastic scattering amplitude, and β is the slope of the hadron-nucleon elastic scattering intensity near the forward direction. If we assume Eq. (2.3) for the form of $f(q)$, Eq. (2.1) reduces to

$$F_{ii}(0)=ik\int_0^\infty\left\{1-\left[1-\frac{(1-i\alpha)\sigma_N}{4\pi}\times\int_0^\infty J_0(qb)e^{-\beta q^2/2}S(q)q\,dq\right]^A\right\}b\,db. \tag{2.4}$$

The hadron-nuclei total cross sections may be obtained from $F_{ii}(0)$ by means of the optical theorem

$$\sigma=(4\pi/k)\,\mathrm{Im}F_{ii}(0) \tag{2.5}$$

$$=4\pi\,\mathrm{Re}\int_0^\infty\left\{1-\left[1-\frac{(1-i\alpha)\sigma_N}{4\pi}\times\int_0^\infty J_0(qb)e^{-\beta q^2/2}S(q)q\,dq\right]^A\right\}b\,db\,. \tag{2.6}$$

III. TOTAL CROSS SECTIONS FOR WOODS-SAXON DENSITY DISTRIBUTIONS AND FOR HARMONIC-OSCILLATOR WAVE FUNCTIONS

In this section we calculate neutron-nuclei total cross sections for a wide variety of nuclei. For the heavier nuclei ($A\geq 27$) we shall assume density distributions of the form

$$A\rho(r)=\frac{C}{1+\exp[(r-R)/a]}\,, \tag{3.1}$$

where C is a normalization constant obtained from the condition

$$\int\rho(r)d\vec{r}=1\,. \tag{3.2}$$

For convenience we also define

$$t=4a\ln 3\,. \tag{3.3}$$

For lighter nuclei ($4\leq A\leq 12$) we shall assume density distributions obtained from an independent-particle harmonic-oscillator model. The single-particle densities are given by

$$\rho(r)=\frac{4}{A}\left(\frac{\gamma^2}{\pi}\right)^{3/2}\left[1+\left(\frac{A}{6}-\frac{2}{3}\right)\gamma^2r^2\right]e^{-\gamma^2r^2}. \tag{3.4}$$

When this expression is substituted into Eq. (2.2) and the result used in Eq. (2.4) we obtain

$$F_{ii}(0)=ik\int_0^\infty\left\{1-\left[1-\frac{(1-i\alpha)\sigma_N\gamma^2}{2\pi(1+2\gamma^2\beta)}\times\left(1-\frac{4B}{A(1+2\gamma^2\beta)}+\frac{4Bb^2\gamma}{A(1+2\gamma^2\beta)^2}\right)\times e^{-\gamma^2b^2/(1+2\gamma^2\beta)}\right]^A\right\}b\,db\,, \tag{3.5}$$

TABLE I. Nuclear parameters together with references.

Target	R (fm)	t (fm)	$\langle r^2\rangle^{1/2}$ (fm)	Reference
He			1.71	32
Li			2.44	44
Be			2.42	41
C			2.47	33
Al	3.07	2.28		34
Fe	3.94	2.5		35
Ni	4.09	2.51		36
Cu	4.16	2.5		35
Zn	4.22	2.50		35
Ag	5.14	2.3		43
Cd	5.21	2.3		43
Sn	5.32	2.53		37
W	6.52	2.16		38
Pb	6.67	2.21		39
Bi	6.73	2.12		40
U	7.11	2.05		38

where

$$B=\frac{A}{6}-\frac{2}{3}. \tag{3.6}$$

Although this integral can be performed analytically, the result is a rather tediously long expression. Alternatively, it can be evaluated quite accurately by standard numerical integration techniques.

In order to obtain qualitative features of the cross sections predicted by our analysis, in our earlier work[18] we used simple parametrizations for R and a in Eq. (3.1) given by Elton.[31] These parametrizations are useful for understanding the gross behavior of the total cross sections as functions of the mass number A. However, in order to treat the nuclei more realistically, it is necessary to consider each nucleus as a different target with values of R and a (or γ) obtained from measurements on that nucleus. In the present analysis the values of R, a, and γ are obtained from electron scattering experiments and from observations of mesonic x rays. (Our calculations, consequently, contain no adjustable parameters.)

In Table I we present the values of R and t used for the heavier nuclei and the values of the rms radii used for the lighter nuclei, together with the references to the measurements[32-44] from which they were obtained. The rms radius is related to γ in Eqs. (3.4) and (3.5) by

$$\langle r^2\rangle=\gamma^{-2}\left(\frac{5}{2}-\frac{2}{Z}-\frac{3}{2A}\right)+a^2, \tag{3.7}$$

where a^2 is the mean square radius of the proton, taken to be 0.726 fm^2,[45] and Z is the atomic number of the target.

In Table II we present the values of σ_N, α, and β used for the basic amplitude $f(q)$ given by Eq. (2.3), together with the references to the measurements[46-65] from which they were obtained. The parameters are the average of proton-proton and neutron-proton data near the incident momentum of interest. The incident momenta listed are those for which neutron-nucleus cross-section data exist.

In Tables III and IV we present the results of our calculations and compare them with the data. Corresponding to a given target and a given momentum, two entries are shown in the tables if

TABLE II. Average nucleon-nucleon parameters together with references.

Momentum (GeV/c)	σ_N (mb)	α	β (GeV/c)$^{-2}$	Reference
26.5	39.1	−0.34	8.79	27, 46, 47, 57
21	38.8	−0.34	8.19	28, 46, 56, 57, 64
18	38.7	−0.33	7.95	24, 27, 46, 48, 57, 58
16	38.9	−0.33	8.64	24, 28, 46, 49, 57, 58
14	38.9	−0.31	8.64	24, 28, 50, 56, 57, 58
13	39.0	−0.35	8.73	27, 49, 50, 58, 59, 65
12	39.4	−0.35	7.66	24, 27, 46, 48, 58, 59
11	39.5	−0.34	8.08	28, 50, 56, 59, 60, 64
9	39.7	−0.32	8.03	21, 50, 56, 59, 61, 64
8	39.9	−0.34	7.26	28, 46, 51, 57, 58, 59
5.7	41.7	−0.40	7.37	19, 29, 52, 53, 59
3.8	42.6	−0.42	7.09	19, 54, 55, 59
2.4	43.4	−0.02	6.25	19, 26, 54, 56, 60, 62
2.14	44.6	−0.32	6.25	19, 54, 56, 59
2.1	43.7	−0.20	6.25	19, 26, 54, 56, 63
1.925	43.3	−0.20	5.97	19, 26, 54, 56, 63
1.775	43.0	−0.20	5.97	19, 26, 54, 56, 63
1.65	42.8	−0.20	6.30	19, 26, 52, 56, 63

measurements exist for that target and momentum. The upper entry is our theoretical prediction and the lower entry is the measured cross section. The measurements at 1.65, 1.775, 1.925, 2.1, and 2.4 GeV/c are by Schimmerling *et al.*[25] Those at 2.14 GeV/c are by Coor *et al.*,[20] and those at 3.8 GeV/c are by Lakin *et al.*[23] At the higher momenta, the measurements at 5.7 GeV/c are by Parker *et al.*,[29] those at 8, 9, 11, 14, 16, and 21 GeV/c are by Engler *et al.*,[21,28] and those at 12, 13, 18, and 26.5 GeV/c are by Jones *et al.*[27]

The predicted results are in good agreement with the data except, perhaps, at 26.5 GeV/c. At this momentum the predictions are systematically high by approximately 4%. It is possible that at this high a momentum the contributions to the forward elastic scattering amplitude which arise from inelastic intermediate states begin to be significant and should be incorporated into the theory.[66] On the other hand, a relatively small discrepancy of 4% can be fully accounted for by the uncertainty in the neutron-nuclei measurements (~2%) and the uncertainties in the measurements of the nuclear (R, t, γ) and nucleon-nucleon $(\sigma_N, \alpha, \beta)$ parameters that enter the calculations.

Since our predictions are made using nuclear and nucleon-nucleon measurements, we have determined the magnitudes of the uncertainties induced in our predictions by uncertainties in the measurements for the parameters R, t, γ, σ_N, α, and β. To obtain a rough estimate of the resulting uncertainties in our predictions, we assume conservative uncertainties of ±0.1 fm in R, ±0.1 fm in t, ±0.7 mb in σ_N, ±0.25 (GeV/c)$^{-2}$ in β, and ±0.04 in α. For $4 \leq A \leq 12$, the uncertainty used for γ was that resulting in an uncertainty of ±0.1 fm in $\langle r^2 \rangle^{1/2}$. In order to exhibit the effect on σ resulting from the separate uncertainties in the parameters, we show in Table V the approximate amount by which the neutron-lead cross-section changes as the result of small independent changes in σ_N, β, γ, t, and R. These uncertainties combine to give a maximum total uncertainty in σ of approximately 110 mb, which is ~3.5% of the total

TABLE III. Predicted and measured neutron-nuclei total cross sections. The upper entries are the predictions. The lower entries are the measured values.

	P (GeV/c)								
Target	1.65	1.775	1.925	2.1	2.14	2.4	3.8	5.7	8
He								141	
								142 ± 3	
Be	293	294	295	298	306	294		296	283
	290 ± 9	307 ± 8	313 ± 8	314 ± 8	308 ± 13	312 ± 9		301 ± 5	282 ± 3
C	357	358	360	362	373	358	369	363	348
	358 ± 7	352 ± 7	380 ± 7	364 ± 7	378 ± 10	371 ± 8	369 ± 7	370 ± 6	356 ± 3
Al	693	694	696	701	721	693	718	708	681
	704 ± 18	689 ± 17	674 ± 19	725 ± 19	703 ± 18	741 ± 25	666 ± 16	718 ± 13	676 ± 5
Fe	1202	1204	1207	1214		1201		1230	
	1181 ± 31	1142 ± 31	1159 ± 32	1180 ± 32		1121 ± 37		1250 ± 20	
Ni	1265	1266	1270	1277		1263			
	1266 ± 21	1235 ± 19	1272 ± 20	1261 ± 19		1265 ± 24			
Cu	1326	1327	1330	1338	1372	1324	1372	1356	1314
	1331 ± 28	1245 ± 25	1303 ± 28	1304 ± 26	1388 ± 39	1325 ± 33	1331 ± 17	1410 ± 30	1339 ± 13
Zn	1357	1358	1362	1369		1355			
	1431 ± 37	1397 ± 34	1436 ± 37	1370 ± 35		1379 ± 40			
Ag	1918	1919	1923	1932		1914			
	1974 ± 50	1887 ± 46	1910 ± 50	1896 ± 47		1904 ± 58			
Cd								2022	
								2120 ± 30	
Sn	2107	2109	2113	2123	2171	2102			
	2119 ± 55	2025 ± 50	2179 ± 54	1952 ± 51	2202 ± 62	2082 ± 63			
W								2973	
								2970 ± 70	
Pb	3110	3111	3116	3128	3188	3102	3199	3177	3108
	3091 ± 77	3016 ± 72	3139 ± 79	3092 ± 78	3209 ± 55	3134 ± 96	3071 ± 79	3240 ± 50	3235 ± 30
Bi	3126	3127	3132	3144	3204	3118			
	3182 ± 92	3028 ± 85	3090 ± 92	3072 ± 89	3275 ± 65	2985 ± 114			
U	3446	3447	3452	3464	3528	3437		3519	
	3440 ± 72	3179 ± 72	3452 ± 79	3448 ± 78	3640 ± 91	3454 ± 102		3620 ± 60	

TABLE IV. Predicted and measured neutron-nuclei total cross sections. The upper entries are the predictions. The lower entries are the measured values.

	P (GeV/c)								
Target	9	11	12	13	14	16	18	21	26.5
He	135								
	141 ± 6								
Li	234								
	236 ± 7								
Be	282	282			278			278	280
	271 ± 6	278 ± 3			277 ± 3			276 ± 8	266 ± 6
C	347	347	346	345	343		341	343	345
	340 ± 3	347 ± 3	342 ± 3	340 ± 3	343 ± 3		342 ± 3	340 ± 8	330 ± 7
Al	679	680			672	674		673	677
	683 ± 3	663 ± 5			655 ± 5	649 ± 9		647 ± 6	656 ± 11
Fe	1187								
	1204 ± 12								
Cu	1310	1313	1309	1309	1299		1297	1302	1308
	1364 ± 14	1295 ± 14	1305 ± 9	1295 ± 8	1295 ± 12		1265 ± 8	1268 ± 14	1251 ± 19
Cd									1964
									1907 ± 32
W									2899
									2720 ± 41
Pb	3102	3109	3103	3106	3087		3084	3093	3104
	3146 ± 50	3138 ± 38	3167 ± 21	3150 ± 19	3140 ± 30		3100 ± 19	3062 ± 30	3044 ± 45

cross section. It is clear from Table V that neutron-nuclei total cross sections are rather sensitive to the skin thickness t and the half-density parameter R. However, unless σ_N and α are accurately known, neutron-nuclei total cross-section measurements could not be used as a means for determining R or t to better than approximately 0.1 or 0.2 fm, respectively. To the extent that the predictions for a given nucleus differ from the data, one might conclude that the density distribution for neutrons differs from that for protons. For example, our predictions for aluminum, iron, and copper would improve if the rms radii of the neutron distributions were slightly smaller than those of the corresponding proton distributions.

In Figs. 1–4 we compare with the data the calculated neutron-nuclei total cross sections for individual targets as functions of the incident neutron momenta. Corresponding figures for nuclei with less data may be obtained from Table I. We also show upper and lower limits on the calculations resulting from the assumed uncertainties discussed previously. We see that the predictions are generally consistent with the measurements. The sharp rise in the predicted cross sections at 2.14 GeV/c is a result of the large value of the n-p cross section obtained[19] for that energy and used in our calculation. That value is more than 2% larger than the value obtained by direct measurements[26] at 2.1 GeV/c.

IV. TOTAL CROSS SECTIONS FOR GAUSSIAN DENSITY DISTRIBUTIONS

In this section we shall consider density distributions of the form

$$\rho(r) = (\pi R^2)^{-3/2} e^{-r^2/R^2}. \tag{4.1}$$

Although such a representation is not at all accurate for most nuclei, we will find that the gross features of the cross-section data are not badly described with Eq. (4.1). Furthermore, since the total cross section can be expressed in a simple analytic form, a number of interesting observations regarding the multiple scattering series may be easily made.

TABLE V. Changes in the neutron-lead total cross sections resulting from changes in parameters used in the calculations.

	$\Delta\sigma$ (mb)
$\Delta\sigma_N = \pm 0.7$ mb	±17
$\Delta\beta = \pm 0.25$ (GeV/c)$^{-2}$	± 2
$\Delta\alpha = \pm 0.04$	±16
$\Delta t = \pm 0.1$ fm	±26
$\Delta R = \pm 0.1$ fm	±51

With Eq. (2.3) for $f(q)$ and with Eq. (4.1) for $\rho(r)$, a straightforward calculation yields

$$\sigma = 2\pi(R^2+2\beta)\,\mathrm{Re}\sum_{l=1}^{A}(-1)^{l+1}\binom{A}{l}\frac{1}{l}\left[\frac{(1-i\alpha)\sigma_N}{2\pi(R^2+2\beta)}\right]^l . \tag{4.2}$$

[A different closed form expression, differing from Eq. (4.2) in terms of order A^{-1}, was obtained by Bethe.[16]]

For heavy nuclei there will be many terms in the series. It is possible to obtain by geometrical considerations a rough estimate of the number of significant terms in the series. Let us imagine the nucleus to consist of A nucleons and let them be distributed uniformly throughout a sphere of radius $R = r_0 A^{1/3}$. The number of nucleons per unit volume is then $A/(4\pi R^3/3) = 3/4\pi r_0^3$. Now at high energies most of the hadron-nucleon collisions within the nucleus will be small-angle collisions, particularly if there is no net deflection. Consequently it is reasonable to expect that in the great majority of cases a hadron would undergo at most that number of collisions it would have experienced had it traversed the nucleus along its diameter. That number is the product of the number of nucleons per unit volume and the effective volume swept out by the hadron as it travels along a nuclear diameter. The effective volume is the product of the diameter $2R$ and the effective cross section σ_N of the hadron. Taking $r_0 = (\frac{2}{5})^{1/2}(1.25)$, the motivation for which we describe in the next section, we obtain $3R\sigma_N/2\pi r_0^3 = (3\sigma_N/2\pi r_0^2)A^{1/3}$ as the number of significant terms in the series. For neutron-nucleon collisions at high energies $\sigma_N \approx 39$ mb, and we obtain

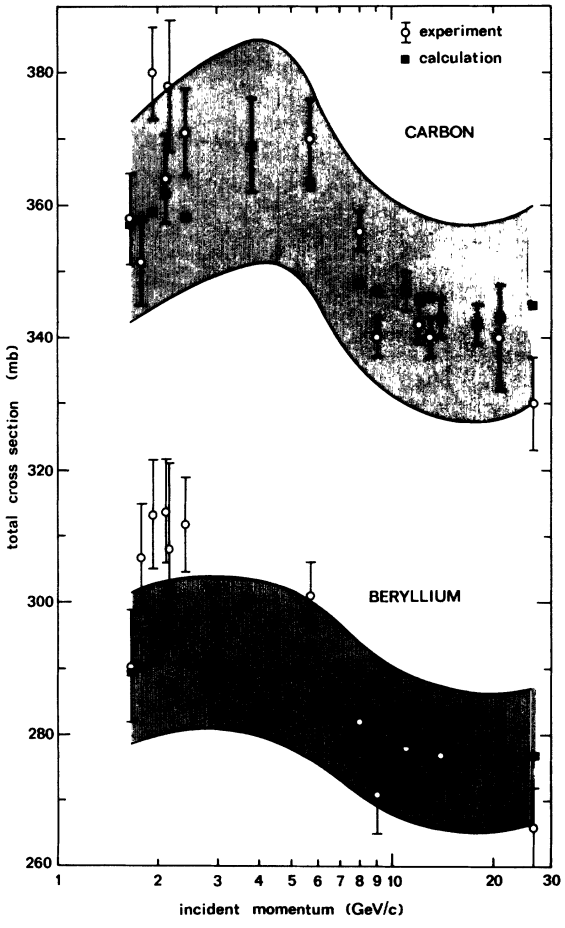

FIG. 1. Neutron-carbon and neutron-beryllium total cross sections as a function of incident momentum. The curves represent the upper and lower limits of the predicted cross sections when specified uncertainties in the input parameters are considered. See text for detailed discussion.

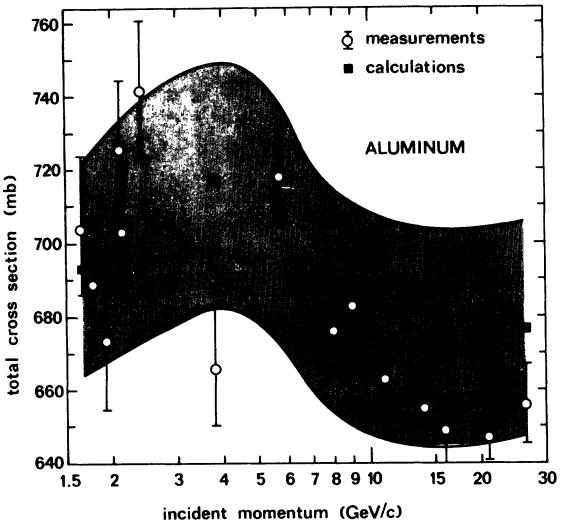

FIG. 2. Same as Fig. 1 for neutron-aluminum total cross sections.

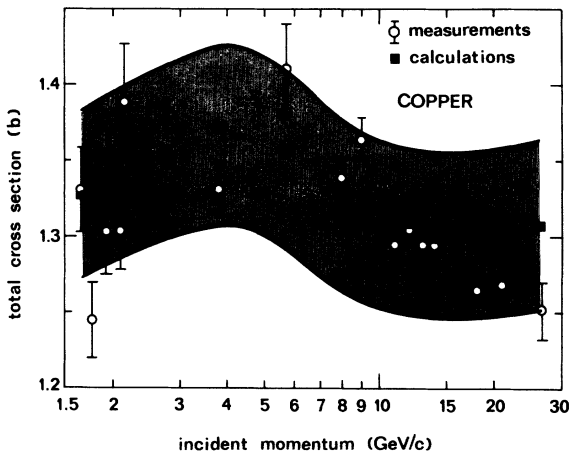

FIG. 3. Same as Fig. 1 for neutron-copper total cross sections.

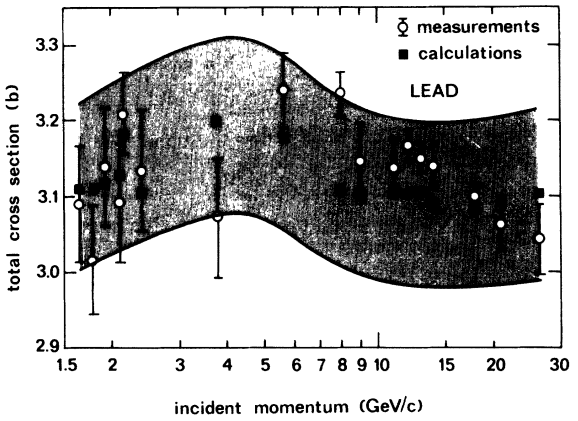

FIG. 4. Same as Fig. 1 for neutron-lead total cross sections.

approximately $3A^{1/3}$ as the number of significant terms in the series for neutron-nucleus cross sections. Thus, even for a heavy nucleus like ^{207}Pb we would expect only approximately the first 18 terms to contribute significantly to the sum, rather than all 207 terms. From numerical calculations we find that for $A=207$, the first 15 terms of the sum contribute ~99.95% of the total cross section and the first 18 terms contribute ~99.995% of the total cross section.

To illustrate some properties of the series (4.2), we rewrite it in the form

$$\sigma(A)=\sum_{l=1}^{A} g_l(A)\,, \tag{4.3}$$

where

$$g_l(A)=2\pi(R^2+2\beta)(-1)^{l+1}\binom{A}{l}\frac{1}{l}\mathrm{Re}\left[\frac{(1-i\alpha)\sigma_N}{2\pi(R^2+2\beta)}\right]^l, \tag{4.4}$$

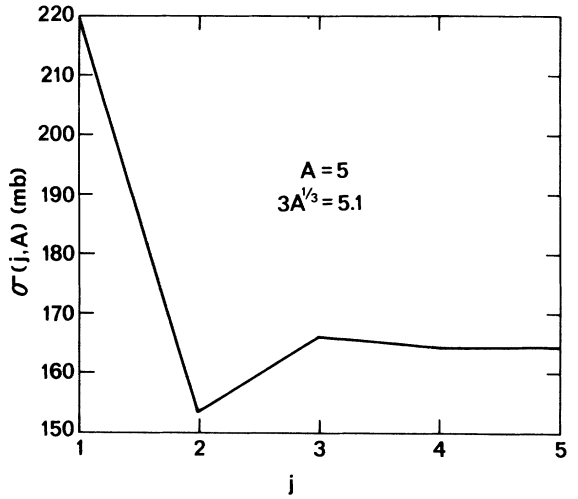

FIG. 5. Partial sums, given by Eqs. (4.4) and (4.5), for an $A=5$ nucleus.

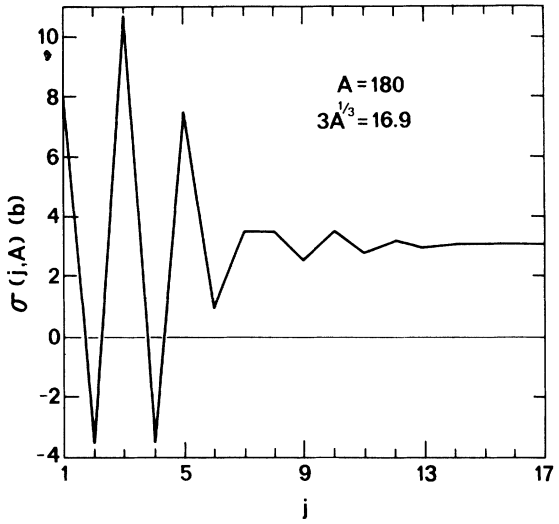

FIG. 6. Partial sums, given by Eqs. (4.4) and (4.5), for an $A=180$ nucleus.

and we define partial sums $\sigma(j,A)$ by the relation

$$\sigma(j,A)=\sum_{l=1}^{j} g_l(A)\,. \tag{4.5}$$

In Figs. 5 and 6 we show $\sigma(j,A)$ as a function of j for 1.7-GeV/c neutrons and $A=5$ and 180. We note from these figures that the series (4.2) converges quite rapidly, requiring roughly $3A^{1/3}$ terms to obtain excellent accuracy. However, we also note that premature truncation of the series would lead to grossly inaccurate and often unmeaningful (i.e., negative) values for the cross sections.

Let us now calculate the total cross sections using Eq. (4.1) for the density distribution. For this density distribution R is related to the rms radius

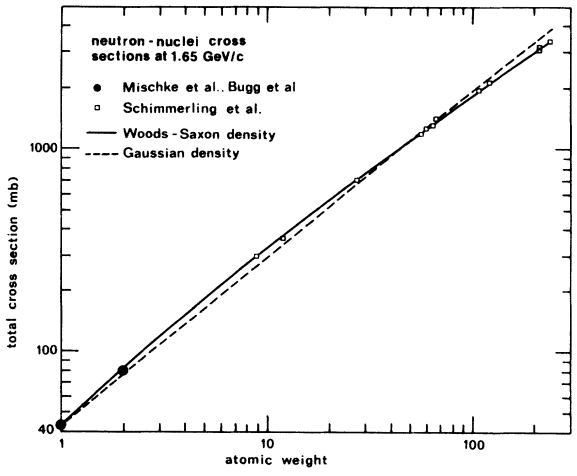

FIG. 7. Neutron-nuclei total cross sections at 1.65 GeV/c as a function of atomic weight. Calculations using Woods-Saxon and Gaussian density distributions are compared with each other and with the measurements.

$\langle r^2\rangle^{1/2}$ by

$$R=\sqrt{\tfrac{5}{3}}\langle r^2\rangle^{1/2}. \tag{4.6}$$

We shall take the variation of the rms radius with mass number A to be that given by a uniform distribution whose half-density radius c is given by the usual $1.25A^{1/3}$ fm obtained in optical-model analyses of nucleon-nucleus collisions. For a uniform charge distribution, $\langle r^2\rangle = 3c^2/5$. Therefore, we obtain

$$R=\sqrt{\tfrac{5}{3}}\,1.25A^{1/3}\text{ fm}. \tag{4.7}$$

The total cross sections are, therefore, given by Eq. (4.2) with R given by Eq. (4.7). How do these cross sections compare with those obtained from a Woods-Saxon density distribution? The qualitative differences are rather insensitive to the incident energy and incident particle. The cross sections obtained with a Gaussian density distribution are lower for A less than approximately 40–60. For larger values of A, the cross sections obtained with a Woods-Saxon density distribution are lower. We illustrate this difference in Fig. 7 where we present the calculations with the two density distributions and the data for neutrons at 1.65 GeV/c. For the Woods-Saxon density distributions we assume that[42] $t=2.3$ fm and $R=(1.18A^{1/3}-0.48)$ fm. We note that the differences between the two curves are relatively small, never exceeding approximately 15% in magnitude. However, the calculation with the Woods-Saxon distribution appears to be in significantly better agreement with the measurements both in the qualitative shape of the curve and in the actual magnitudes, than does the calculation with the Gaussian distribution. The A dependence of the total cross section is predicted quite accurately with the Woods-Saxon distribution.

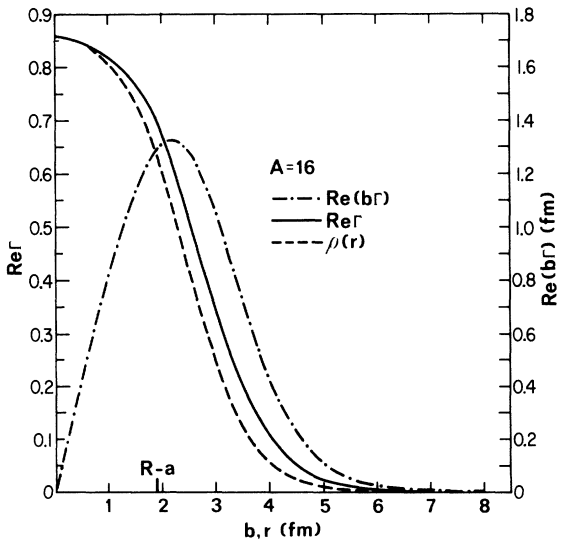

FIG. 8. Woods-Saxon density distribution $\rho(r)$, $\mathrm{Re}\Gamma(b)$, and $\mathrm{Re}[b\Gamma(b)]$ for an $A=16$ nucleus.

V. NUCLEAR DENSITY DISTRIBUTIONS

We have seen that the total cross sections obtained with Woods-Saxon density distributions may differ by as much as 15% from those obtained from Gaussian distributions. To that extent total cross-section measurements may be used to investigate nuclear density distributions. Is there any region of the nucleus to the density of which the total cross sections are most sensitive? To investigate this question we write

$$\Gamma(b)=1-\left[1-\frac{1}{ik}\int_0^\infty J_0(qb)f(q)S(q)q\,dq\right]^A. \tag{5.1}$$

If we refer to Eq. (2.1) we see that the total cross section is given by

$$\sigma=4\pi\int_0^\infty \mathrm{Re}[b\Gamma(b)]db.$$

Thus we may think of $4\pi\,\mathrm{Re}[b\Gamma(b)]$ as the contribution per unit length of impact parameter to the total cross section at the impact parameter b.

In Figs. 8 and 9 we show $\mathrm{Re}[b\Gamma(b)]$ as a function of b for several values of the atomic weight A. The Woods-Saxon density distributions described earlier are used for these calculations and are also shown in the figures. We note that $\mathrm{Re}[b\Gamma(b)]$ attains its maximum value for $b\approx R-a$. Near this impact parameter the effect of decreasing density is most effectively compensated for by the large cross-sectional area presented to the incident beam. The values of r which contribute to this maximum are therefore $r\gtrsim R-a$, which constitute the surface and outer regions of the nucleus. However, although the outer regions of the nucleus are being probed most by total cross-section measurements, it is important to bear in mind that the other regions of the nucleus also contribute significantly to the cross sections.

In Figs. 8 and 9 we also show the behavior of

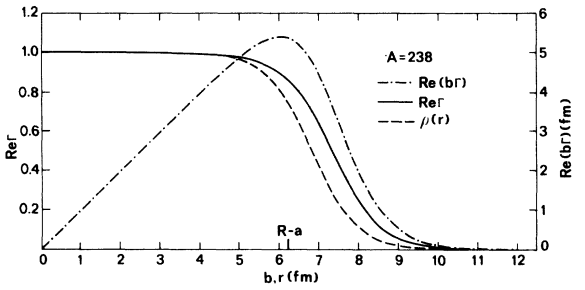

FIG. 9. Woods-Saxon density distribution $\rho(r)$, $\mathrm{Re}\Gamma(b)$, and $\mathrm{Re}[b\Gamma(b)]$ for an $A=238$ nucleus.

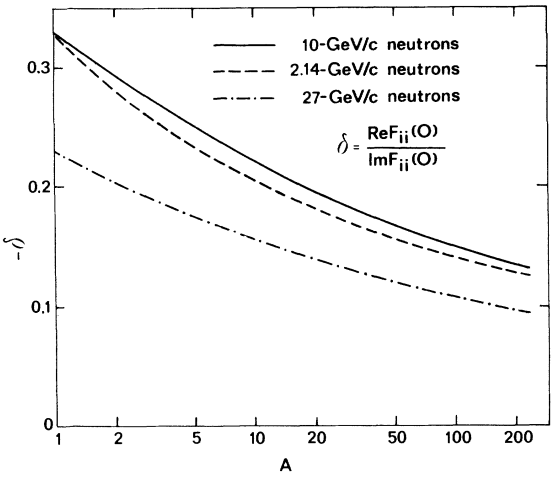

FIG. 10. The variations with mass number of the ratios of the real parts to the imaginary parts of neutron-nucleus forward elastic scattering amplitudes.

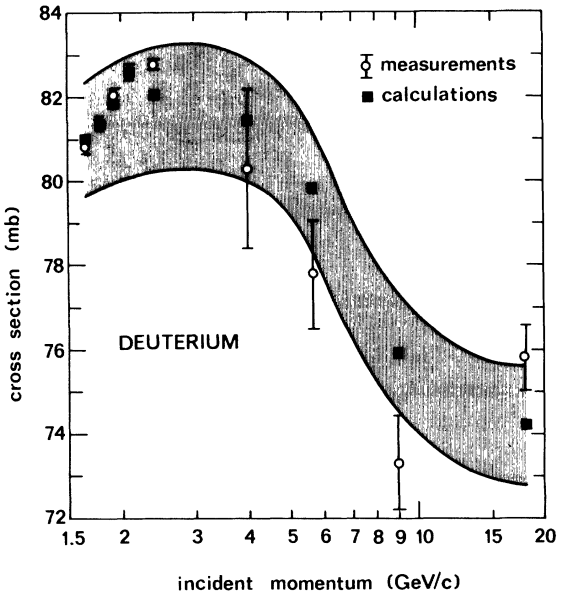

FIG. 11. Same as Fig. 1 for neutron-deuterium total cross sections.

$\mathrm{Re}\Gamma(b)$ which we note is quite similar to that of the density distribution $\rho(r)$. Since $\rho(r)$ does not possess a sharp cutoff, and since $\mathrm{Re}\Gamma$ decreases even more slowly from its value at $b=0$ than does $\rho(r)$ from its value at $r=0$, σ should increase with A more rapidly than $A^{2/3}$. This is indeed what is found experimentally. The data can be fairly well approximated by an $A^{0.82}$ dependence. However, for heavy nuclei since, as can be seen from Fig. 9, $\Gamma(b)\approx 1$ over a large range of value of b and the bulk of the cross section comes from these values of b, the cross sections will increase at a rate closer to $A^{2/3}$. This decrease in the slopes of the σ vs A curves is readily observed in Fig. 7 where the curves possess negative second derivatives.

VI. REAL PAIRS OF HADRON-NUCLEI FORWARD ELASTIC SCATTERING AMPLITUDES

A feature of hadron-nucleon collisions above ~1 GeV/c is that α, the ratio of the real to imaginary parts of the forward elastic scattering amplitude,

TABLE VI. Neutron-deuteron total cross sections.

Momentum (GeV/c)	σ(theor.) (mb)	σ(exp.) (mb)
1.65	81.00	80.83 ± 0.17
1.775	81.37	81.37 ± 0.18
1.925	81.83	82.02 ± 0.19
2.1	82.60	82.61 ± 0.18
2.4	82.02	82.78 ± 0.12
4.0	81.5	80.3 ± 1.9
5.7	79.8	77.8 ± 1.3
9	75.9	73.3 ± 1.1
18	74.2	75.8 ± 0.8

is considerably smaller in magnitude than unity. Let us define the corresponding ratios, δ, for hadron-nuclei elastic scattering amplitudes,

$$\delta = \mathrm{Re}F_{ii}(0)/\mathrm{Im}F_{ii}(0)$$
$$= \delta(A).$$

For $A=1$, we have $\delta(1)=\alpha$. It would be useful to determine how δ depends upon A.

Since high-energy interactions with nuclei are likely to be more absorptive for heavier nuclei than for lighter nuclei, we would expect the magnitude of δ to decrease with increasing A. In Fig. 10 we show $\delta(A)$ for several different incident energies. These curves were calculated using the density given by Eq. (4.1). We note the expected decrease in $|\delta|$ with increasing A. For $A \gtrsim 60$ the magnitude of δ has decreased to less than one half the magnitude of α [i.e., $\delta(1)$].

VII. NEUTRON-DEUTERON CROSS SECTIONS

There exist a number of detailed analyses of hadron-deuteron collisions. To obtain predictions for neutron-deuteron total cross sections we apply the optical theorem to the hadron-deuteron elastic scattering amplitudes derived by Franco and Glauber.[5] The s- and d-state wave functions we use are those given by Moravcsik.[67] In Table VI we compare the calculated values with the data. In Fig. 11 we exhibit the momentum dependence of the predicted deuteron cross sections and compare it with the measurements.

ACKNOWLEDGMENT

We wish to thank Dr. R. E. Mischke for making some data available prior to publication and for his analysis of the uncertainties in the data at 2.4 GeV/c.

*Work supported in part by the National Science Foundation and by the City University of New York Faculty Research Award Program.

[1]V. Franco and R. J. Glauber, Phys. Rev. 142, 1195 (1966).

[2]V. Franco, Ph.D. thesis, Harvard University, 1963 (unpublished).

[3]V. Franco, Phys. Rev. Letters 16, 944 (1966).

[4]V. Franco and E. Coleman, Phys. Rev. Letters 17, 827 (1966).

[5]D. R. Harrington, Phys. Rev. Letters 21, 1496 (1968); V. Franco and R. J. Glauber, Phys. Rev. Letters 22, 370 (1969).

[6]E. Kujawski, D. Sachs, and J. Trefil, Phys. Rev. Letters 21, 583 (1968).

[7]V. Franco, Phys. Rev. Letters 21, 1360 (1968).

[8]H. C. Hsuing *et al.*, Phys. Rev. Letters 21, 187 (1968).

[9]M. Fellinger *et al.*, Phys. Rev. Letters 22, 1265 (1969).

[10]F. Bradamante *et al.*, Phys. Letters 28B, 193 (1968).

[11]G. W. Bennett *et al.*, Phys. Rev. Letters 19, 387 (1967).

[12]E. T. Boschitz *et al.*, Phys. Rev. Letters 20, 1116 (1968).

[13]R. J. Glauber, in *Lectures in Theoretical Physics*, edited by W. E. Brittin *et al.* (Interscience, New York, 1959), Vol. I.

[14]R. A. Rudin, Phys. Letters 30B, 357 (1969); A. Y. Abul-Magd, Nucl. Phys. B8, 938 (1968).

[15]Neutron-nucleus total cross sections at lower energies have been calculated by means of an eikonal approximation by V. Franco, Phys. Rev. 140, B1501 (1965), who used square well and Woods-Saxon optical potentials to represent the nuclear interactions.

[16]N. C. Francis and K. M. Watson, Phys. Rev. 92, 291 (1953); H. A. Bethe, Ann. Phys. (N.Y.) 3, 190 (1958); and A. Kerman, H. McManus, and R. Thaler, Ann. Phys. (N.Y.) 8, 551 (1959).

[17]V. Franco, Phys. Rev. 175, 1376 (1968).

[18]A. brief description of some of this analysis was given by V. Franco, Phys. Rev. Letters 24, 1452 (1970).

[19]D. V. Bugg *et al.*, Phys. Rev. 146, 980 (1966).

[20]T. Coor *et al.*, Phys. Rev. 98, 1369 (1955).

[21]J. Engler *et al.*, Phys. Letters 27B, 599 (1968); and 28B, 64 (1968).

[22]M. N. Kreisler, L. W. Jones, M. J. Longo, and J. R. O'Fallon, Phys. Rev. Letters 20, 468 (1968).

[23]W. L. Lakin *et al.*, Phys. Letters 31B, 677 (1970).

[24]W. Galbraith *et al.*, Phys. Rev. 138, B913 (1965).

[25]W. Schimmerling *et al.*, Phys. Letters 37B, 177 (1971).

[26]R. E. Mischke *et al.*, Phys. Rev. Letters 25, 1724 (1970).

[27]L. W. Jones *et al.*, Phys. Letters 36B, 509 (1971).

[28]J. Engler *et al.*, Phys. Letters 31B, 669 (1970); and 32B, 716 (1970).

[29]E. F. Parker *et al.*, Phys. Letters 31B, 246 (1970).

[30]E. F. Parker *et al.*, Phys. Letters 31B, 250 (1970).

[31]L. R. B. Elton, *Nuclear Sizes* (Oxford U. P., London, 1961).

[32]R. F. Frosch, J. S. McCarthy, R. E. Rand, and M. R. Yearian, Phys. Rev. 160, 874 (1967).

[33]H. Crannell, Phys. Rev. 148, 1107 (1966).

[34]R. M. Lombard and G. R. Bishop, Nucl. Phys. A101, 601 (1967).

[35]H. Theissen, H. Fink, and H. A. Bentz, Z. Physik 231, 475 (1970).

[36]L. R. B. Elton and A. Swift, Proc. Phys. Soc. (London) 84, 125 (1964).

[37]P. Barreau and J. B. Bellicard, Phys. Letters 25B, 470 (1967).

[38]S. A. DeWitt *et al.*, Nucl. Phys. 87, 657 (1967).

[39]H. L. Acker *et al.*, Nucl. Phys. 87, 1 (1966).

[40]G. J. C. Van Niftrik and R. Engfer, Phys. Letters 22, 490 (1966).

[41]H. Nguyen-Ngoc, Ph.D. thesis, Masson, Paris, 1964 (unpublished).

[42]H. R. Collard, L. R. B. Elton, and R. Hofstadter, in *Landolt-Bornstein: Numerical Data and Functional Relationships in Science and Technology*, edited by H. Schopper (Springer-Verlag, Berlin, 1967), New Series, Group I, Vol. II.

[43]For these elements we have used the empirical fit $t = 2.3$ fm and $R = (1.18A^{1/3} - 0.48)$ fm given in Ref. 42.

[44]G. R. Bishop and M. Bernheim, private communication to H. R. Collard and R. Hofstadter in Ref. 42.

[45]T. Janssens, R. Hofstadter, E. B. Hughes, and M. R. Yearian, Phys. Rev. 142, B922 (1966).

[46]B. G. Gibbard *et al.*, Phys. Rev. Letters 24, 22 (1970).

[47]P. Breitenlohner *et al.*, Phys. Letters 7, 73 (1963).

[48]D. Harting *et al.*, Nuovo Cimento 38, 60 (1965).

[49]G. G. Beznogikh *et al.*, Phys. Letters 30B, 274 (1969).

[50]J. Engler *et al.*, Phys. Letters 29B, 321 (1969).

[51]J. Ginestet, D. Manesse, Tran Ha Anh, and D. Vignaud, Nucl. Phys. B13, 283 (1969).

[52]M. N. Kreisler *et al.*, Phys. Rev. Letters 16, 1217 (1966).

[53]G. Alexander *et al.*, Phys. Rev. 154, 1284 (1967).

[54]M. L. Perl, J. Cox, M. J. Longo, and M. N. Kreisler, Phys. Rev. D 1, 1857 (1970).

[55]S. Colleti *et al.*, Nuovo Cimento 49A, 479 (1967).

[56]O. Benary, L. R. Price, and G. Alexander, UCRL Report No. UCRL-20000NN, 1970 (unpublished).

[57]G. Bellettini *et al.*, Phys. Letters 14, 164 (1965).

[58]K. J. Foley *et al.*, Phys. Rev. Letters 15, 45 (1965).

[59]D. V. Bugg *et al.*, Phys. Rev. 146, 980 (1966).

[60]L. Kirillova *et al.*, Phys. Letters 13, 93 (1964).

[61]L. F. Kirillova *et al.*, Yadern Fiz. 1, 533 (1965) [transl.: Soviet J. Nucl. Phys. 1, 379 (1965)].

[62]L. S. Zolin *et al.*, Zh. Eksperim. i Teor. Fiz. – Pis'ma Redakt. 3, 15 (1966) [transl.: Soviet Phys.–JETP Letters 3, 8 (1966)].

[63]L. M. C. Dutton, R. J. W. Howells, J. S. Jafar, and H. B. Van der Raay, Phys. Letters 25B, 245 (1967).

[64]K. J. Foley *et al.*, Phys. Rev. Letters 19, 857 (1967).

[65]A. Ashmore, G. Cocconi, A. N. Diddens, and A. M. Wetherell, Phys. Rev. Letters 5, 576 (1960).

[66]J. Pumplin and M. Ross, Phys. Rev. Letters 21, 1778 (1968).

[67]M. J. Moravcsik, Nucl. Phys. 7, 113 (1958).

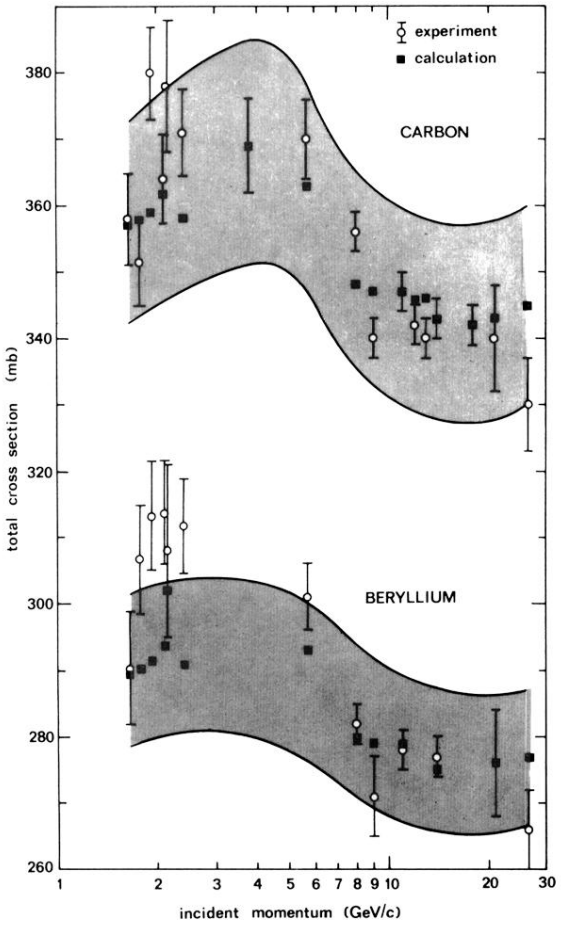

FIG. 1. Neutron-carbon and neutron-beryllium total cross sections as a function of incident momentum. The curves represent the upper and lower limits of the predicted cross sections when specified uncertainties in the input parameters are considered. See text for detailed discussion.

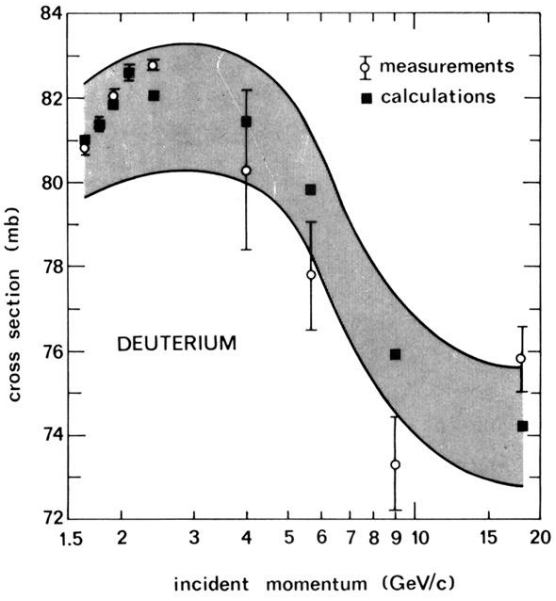

FIG. 11. Same as Fig. 1 for neutron-deuterium total cross sections.

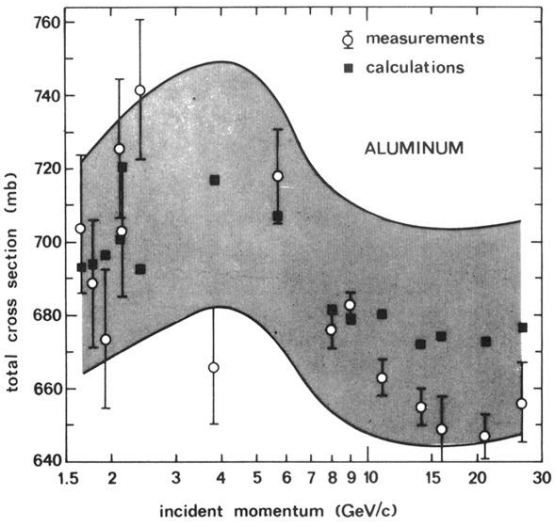

FIG. 2. Same as Fig. 1 for neutron-aluminum total cross sections.

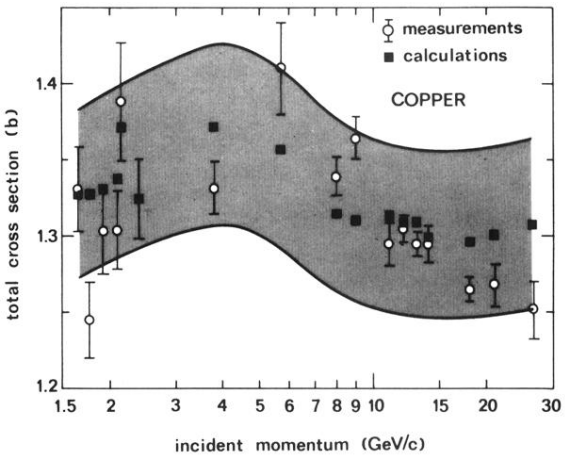

FIG. 3. Same as Fig. 1 for neutron-copper total cross sections.

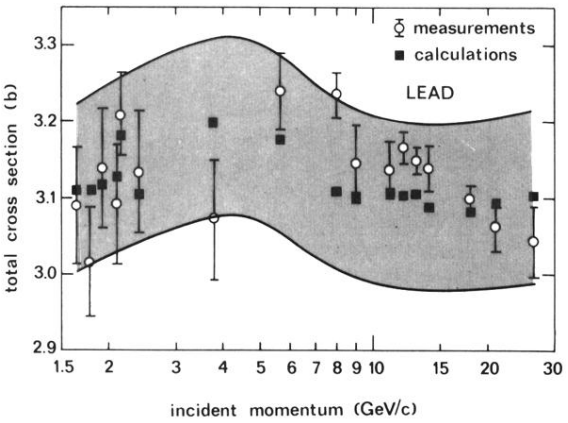

FIG. 4. Same as Fig. 1 for neutron-lead total cross sections.